SCIENCE CHINA
Earth Sciences

• RESEARCH PAPER •

July 2016 Vol.59 No.7: 1390–1400
doi: 10.1007/s11430-015-5239-7

Holocene vegetation succession and responses to climate change in the northern sector of Northeast China

ZHAO Chao[1,2], LI XiaoQiang[1*], ZHOU XinYing[1], ZHAO KeLiang[1] & YANG Qing[3]

[1] *Key Laboratory of Vertebrate Evolution and Human Origins of Chinese Academy of Sciences, Institute of Vertebrate Paleontology and Paleoanthropology, Chinese Academy of Sciences, Beijing 100044, China;*
[2] *University of Chinese Academy of Sciences, Beijing 100049, China;*
[3] *School of Geography Science, Nanjing Normal University, Nanjing 210023, China*

Received June 19, 2015; accepted September 11, 2015; published online March 31, 2016

Abstract Sediment pollen samples from the Huola Basin in the northern sector of northeast China, and surface pollen samples from its environs, were analyzed to reconstruct accurately the historical response of vegetation to climate change since 9100 cal yr BP. Pollen analysis of the Huola Section indicates that vegetation experienced a transformation from early-mid Holocene warm-cold mixed vegetation to late Holocene cold-temperate vegetation. From 9100 to 6000 cal yr BP, the study area was warmer and moister than at present, developing *Corylus*, *Carpinus*, *Pinus*, *Picea*, *Betula* and *Larix*-dominated forests. Two cooling events at 6000–5000 and 3500–2500 cal yr BP led to a decrease in *Corylus*, *Carpinus* and other warmth-loving vegetation, whereas cold temperate forests composed of *Larix* and *Betula* expanded. After 2500 cal yr BP, *Larix* and *Betula* dominated cold-temperate vegetated landscapes. The Holocene warm period in NE China (9100–6000 cal yr BP) suggests that such warming could have resulted in a strengthening of the influence from East Asian Summer Monsoon on northernmost NE China and would have benefited the development of warm-temperate forest vegetation and an improved plant load, which also provides the similarity model for the possible global warming in the future.

Keywords Holocene, Vegetation responses, Cold temperate forest, Northeast China

Citation: Zhao C, Li X Q, Zhou X Y, Zhao K L, Yang Q. 2016. Holocene vegetation succession and responses to climate change in the northern sector of Northeast China. Science China Earth Sciences, 59: 1390−1400, doi: 10.1007/s11430-015-5239-7

1. Introduction

In tackling core issues based on climate change, it is very important to evaluate the effects of climate change accurately (Ding et al., 2009; IPCC, 2013). The Holocene is the most recent geological epoch. It has experienced the increased temperatures of the early Holocene, the warm and humid mid-Holocene, and the cooling of the late Holocene (An et al., 2000; Wang et al., 2005), providing an ideal model for forecasting future climate change. Vegetation succession responded profoundly to climate change in the Holocene; to explore the relationship between vegetation and climate change in critically-affected areas has thus become an important tool in assessing the likely environmental impact of future climate change.

The northern Greater Khingan Range (GKR), in the northernmost part of northeast (NE) China, is located on the eastern margin of the Eurasian continent and contains cold-temperate coniferous forest. It lies in the transition zone between temperate and boreal forest, and between forest and steppe, on the margins of the East Asian Summer Monsoon (EASM) region. It is therefore extremely sensitive to changes in temperature and moisture (Wu et al., 2012).

*Corresponding author (email: lixiaoqiang@ivpp.ac.cn)

Over the past few decades, temperatures in the GKR region have increased, whilst precipitation has decreased, profoundly affecting the growth of larch and other trees, and even the stability of the forest (Chen, 1997). Sub-boreal forests, and especially their dominant tree species (pine, larch, and so forth) have suffered severe withdrawal northward (Guo et al., 2010; Wu et al., 2012). Simulated generalized additive model (GAM) results confirm that, if this process continues, *Larix gmelinii* will disappear from China in 2100 (Li et al., 2006). This research allows us to predict future trends in vegetation in the northern GKR.

Research into the Holocene environment in NE China has focused more on climatic and environmental reconstruction (Ren, 1999, 2007), concentrated on the Sanjiang Plains to the northeast (Zhang et al., 2004; Li et al., 2005; Gao et al., 2014), the Changbai Mountains to the east (Jiang et al., 2008; Hong Y T et al., 2009; Hong B et al., 2009; Mao et al., 2009; Stebich et al., 2009; Li et al., 2011; Zhu et al., 2013; Xu et al., 2014), Hulun Lake to the west (Wen et al., 2010a, 2010b), Dali Lake (Xiao et al., 2008) and Moon Lake (Liu et al., 2010; Wu et al., 2012) and so forth. Xia (1996) has documented the vegetation history of the northern GKR from 2700 cal yr BP. However, a longer vegetation history is needed to verify the successional vegetation responses to climate change in this area.

Pollen is a reliable indicator widely used in the reconstruction of paleovegetation and paleoclimate (Kröpelin et al., 2008; Xu et al., 2014). Understanding the relation between modern pollen and vegetation is a prerequisite for interpreting fossil pollen records correctly, and further improving the accuracy of past vegetation type and paleoclimate reconstruction (Zheng et al., 2008; Zhao and Herzschuh, 2009; Xu et al., 2012). To this effect, we collected topsoil samples covered by different vegetation types in the GKR. Consequently, this study focuses on a typical cold-temperate coniferous forest area dominated by *Larix gmelinii*, based on the high resolution pollen records of Holocene lake-swamp deposition, aims to reconstruct a vegetation succession history, explore successional vegetation responses to climate change (especially during the Holocene megathermal), and provide evidence for the evaluation of the possible effects of future climate change and any necessary adaptation strategies.

2. Study area

The northern GKR (52°32′–53°41′N, 121°15′–125°58′E), which belongs to the permafrost zone, is situated in the northernmost part of China (Figure 1). This area is located in the transition zone between a semi-humid and semi-arid cold-temperate continental monsoon climate; it is controlled by the cold Siberian-Mongolian High (extremely cold and dry) in winter, and is marginally affected by the Pacific High (warm and humid) in summer (Zhou, 1997). Mean annual temperature (MAT) is –4.9°C, minimum temperature is –52.3°C, and the ground is frozen for up to eight months per annum. Mean annual precipitation (MAP) is 403.4 mm, about 80% of which is concentrated in June-September; annual evaporation is about 1000 mm (Guo et al., 1981; Wang et al., 2005).

The GKR has been directly administered by the central government since the Yuan Dynasty (1206–1368 CE) (Feng, 1979; Lan, 2002). Its native inhabitants continued to fish, hunt and gather until the onset of the Opium Wars (1840 CE), when its forests began to undergo large-scale exploitation and utilization (Zhu, 1992; Zhou, 1997). Hence, overall, the Holocene vegetation succession in the study area has been principally affected by natural factors such as climate and environment, with relatively weak human influence (Ren, 2000). It is the ideal area to study vegetation succession and its response to climate change.

At present, the northern GKR contains cold-temperate coniferous forest with *Larix gmelinii* as a typical vegetation type. It belongs to the southernmost tip of the coniferous forest zone that traverses northern Eurasia (Wu, 1979). The study area is located in a region of low-altitude mountains. Its piedmont slopes are covered by mixed coniferous and deciduous forest, including *Larix gmelinii*, *Betula platyphylla*, *Pinus sylvestris* var. *mongolica*, *Quercus mongolica*, *Picea*, *Abies*, *Vaccinium vitis-idaea*, *Betula*, *Salix*, and *Corylus*, and its basins are overgrown with bushes, like Poaceae, *Sanguisorba parviflora* and other meadow weeds (Zhou, 1997; Editorial committee of vegetation map of China, Chinese Academy of Sciences, 2007).

3. Materials and methods

3.1 Surface pollen sampling

Nine topsoil samples were collected from areas covered by different vegetation types in the GKR, according to the 5-point sampling method. We sampled from the center across a 0.5 m radius quadrat and mixed the samples evenly. The samples were mainly mosses, or, in the absence of mosses, gathered lichens or litters. We observed the vegetation type and constructive species within 100 m of the site in range, and estimated the arbor, shrub and herb coverage (Table 1).

3.2 Huola Section samples

The Huola Basin (52.9847°–53.0750°N, 121.9042°–122.0500°E) is one of several low mountain basins in the northern GKR, located about 50 km to the west of Mohe County, and covering an area of 60 km^2, with an average altitude of 720 m a.s.l. for the mountains surrounding the basin, and a relative elevation between them of <200 m (Wang and Lin, 1987; Wang et al., 1988; Guo et al., 1989).

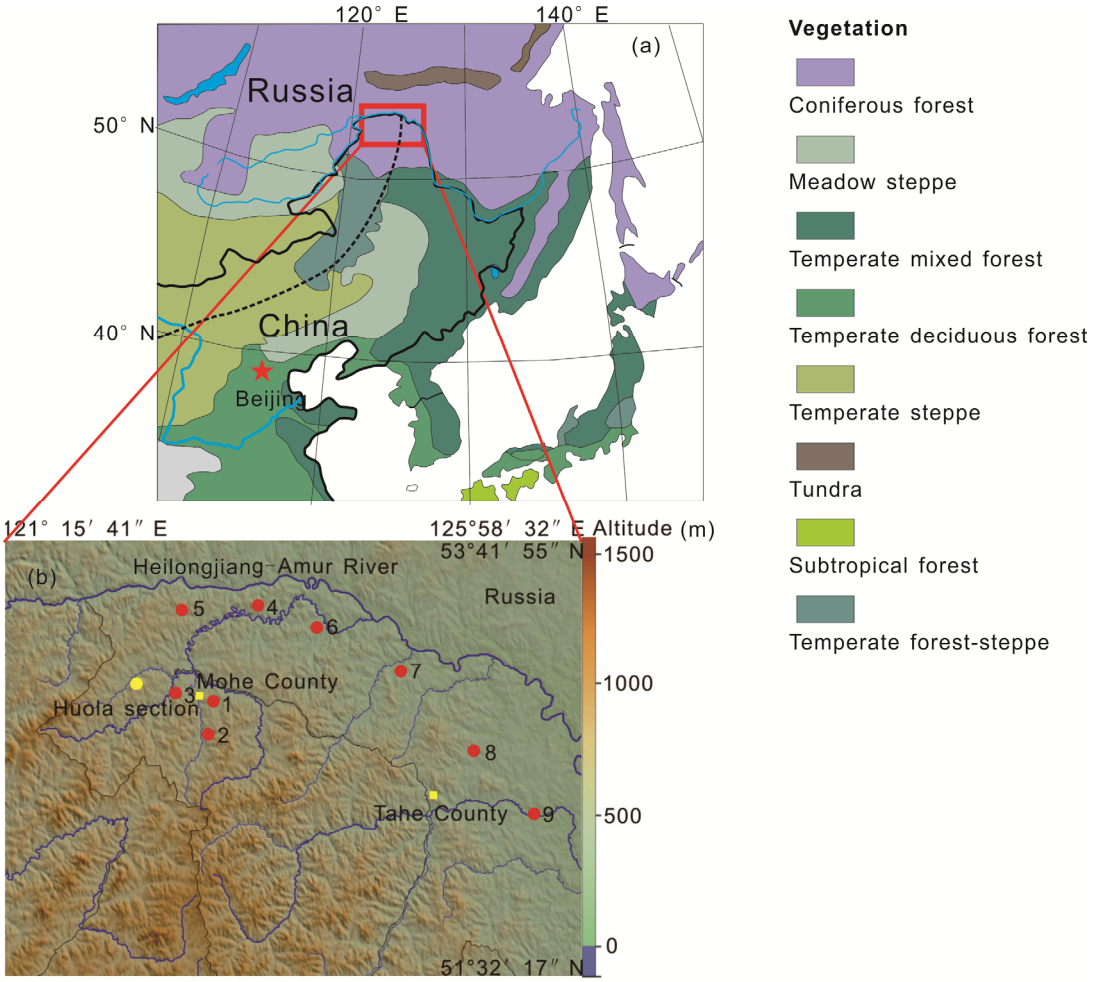

Figure 1 Vegetation map of the study area showing major biomes (Editorial committee of vegetation map of China, Chinese Academy of Sciences, 2007). (a) Red rectangle indicates the study area. Eastern monsoonal margin zone is shown as dotted black line (Zhao et al., 2009). (b) Yellow dot shows the Huola Section; red dots represent surface pollen collections sites; yellow squares indicate counties.

Table 1 Locations of surface pollen sampling points and their vegetative conditions

Sample	Latitude (N)	Longitude (E)	Altitude (m a.s.l.)	Vegetation type and constructive species
1	52°56′18.1″	122°39′51.7″	502	*Larix* forest: *Larix*, *Pinus sylvestris* var. *mongolica*, *Betula platyphylla*, *Picea*, *Alnus*, *Salix hsinganica*, *Vaccinium uliginosum*
2	52°47′16.3″	122°37′32.8″	503	*Betula platyphylla* forest: *Betula platyphylla*, *Larix*, *Alnus*
3	52°59′8.07″	122°15′23.89″	477	*Salix hsinganica* shrub: *Salix hsinganica*, *Alnus*, *Vaccinium uliginosum*
4	53°22′51.6″	123°04′42.8″	525	*Betula platyphylla* and *Larix* mixed forest: *Betula platyphylla*, *Larix*
5	53°19′44.7″	122°19′19.4″	515	*Larix* forest: *Larix*, *Betula platyphylla*
6	53°18′19.5″	123°36′09.4″	147	*Alnus* forest: *Alnus*, *Betula platyphylla*, *Larix*
7	53°08′37.5″	124°18′59.9″	291	*Pinus sylvestris* var. *mongolica* forest: *Pinus sylvestris* var. *mongolica*, *Pinus koraiensis*
8	52°42′21.1″	125°01′22.0″	389	Marsh scrub: *Vaccinium uliginosum*, *Deyeuxia angustifolia*
9	52°23′41.8″	125°29′23.9″	304	Mixed coniferous and deciduous forest: *Quercus*, *Betula platyphylla*, *Larix*, *Alnus*, *Vaccinium uliginosum*

River networks develop in Huola Basin, with the main water from Huolapen River. The Yueya Lake, which is about 0.09 km^2, lies in the south of the basin, surrounding by gleying peat bogs (Wang and Lin, 1987; Li et al., 2010).

The Huola Section (53.0108°N, 121.9634°E, altitude: 535 m a.s.l.) is located in the center of the basin. The 210 cm-long core is delineated as follows: 0–70 cm, brown peat layer; 70–115 cm, yellow lacustrine clay; 115–185 cm, yellow green lacustrine clay; 185–200 cm, turquoise lacustrine clay; 200–201 cm, yellow lacustrine clay. The lithologies of Huola Section are mainly lake-peat facies, indicating a relatively stable sedimentary record.

3.3 Chronology

Five charcoal samples were examined under a steremicroscope to obtain an accurate age-depth framework, rendering depths of 19, 121, 139, 161 and 187 cm (Table 2). AMS ^{14}C dating was conducted at the Australian Nuclear Science and Technology Organization, Australia. Radiogenic ^{14}C ages were recalculated using OxCal4.2.4 and IntCal13, and an age-depth model was produced using OxCal4.2.4 (Ramsey and Lee, 2013; Reimer et al., 2013) (Figure 2). The Huola Section shows a positive correlation between age and depth, although at 139 cm the age is younger than the upper 121 cm section by 10 years. The charcoal at 139 cm may have been disturbed by upper plant residues, such as plant roots and twigs.

A chronosequence for the Huola Section was established using linear interpolation and extrapolation methods based on four samples (taken from 19, 121, 161 and 187 cm depths), with the 139 cm-depth sample left temporarily unconsidered. The section base (210 cm) age was calculated as 9100 cal yr BP. Consequently, the Huola Section represents a set of relatively complete sediments covering the early Holocene period.

3.4 Pollen analysis methods

A total of 62 samples were prepared for pollen analysis, including 53 samples taken at 4cm intervals from the Huola Section, and 9 surface pollen samples. Pollen samples were prepared from sediment samples weighing 3–5 g using conventional acid-alkali treatment and heavy liquid separation (Feagri and Iversen, 1989; Li and Du, 1999), and then further treated by acetolysis (Erdtman, 1960). Lycopodium tablets were added to the samples in order to estimate pollen concentration. Five samples contained 300–400 pollen grains; the remaining samples contained at least 400 pollen grains. Over 60 plant taxa were identified. Pollen percentages and concentrations were calculated with regard to the total sum of terrestrial pollen.

TILIA software was used to draw the pollen spectra, in which a CONISS module was given to calculate distances and cluster zoning based on the square root transformation of the pollen percentage data. Principal component analysis (PCA) was applied to the terrestrial pollen percentage data to extract the main gradient changes in vegetation. The PCA figures were created by CANOCO 4.5 based on both samples and the terrestrial pollen taxa of relative abundance >2%. SPSS version 20.0 was used to generate the PCA F1 and F2 values, showing more comprehensive information on the environment.

4 Results

4.1 Modern pollen assemblages

About 5277 pollen grains were identified, belonging to 42 families and genera. The most abundant arboreal pollen taxa included *Pinus*, *Picea*, *Larix*, Cupressaceae, *Quercus*, *Betula*, *Corylus*, *Carpinus*, *Salix*, *Populus*, *Ulmus*, *Alnus*, and so forth; shrub and herb pollen taxa primarily included Ericaceae, *Artemisia*, Chenopodiaceae, Poaceae, Leguminosae, *Thalictrum*, Compositae, Rosaceae, *Sanguisorba*, Liliaceae, *Plantago*, Apiaceae, Alismataceae, etc. (Figure 3).

In coniferous and broadleaved mixed (CBM) forest, *Betula* (52.30%), *Alnus* (10.69%) and other broadleaved tree pollens dominated modern pollen assemblages. However, *Larix* (4.28%), *Picea* (3.95%) and other coniferous tree pollen were relatively few; *Quercus* (1.64%) and Ericaceae (4.11%) pollen percentages were relatively high.

In *Larix* forest, *Larix* pollen accounted for 1.94–7.32% of the total, significantly lower than its actual proportion in the plant community. However, *Betula* (41.29–46.76%), *Alnus* (40.65–31.45%) and other broadleaf tree pollens were higher in proportion.

Betula (39.45–45.14%) and *Alnus* (17.61–27.43%) pollen dominated modern pollen assemblages in white birch and larch mixed forest. *Larix* pollen content (7.55–14.68%) reached its peak in this environment.

The *Betula* pollen percentage (45%) was also high in *Pinus sylvestris* var. *mongolica* forest. Coniferous pollen content appeared to peak, and, including *Picea* pollen, reached 17.80%.

In alder forest, *Alnus* pollen content accounted for 14.33% of the total, lower than its actual proportion in the plant community, with *Betula* content up to 38.98%, and relatively high herb pollen content (23.42%).

In willow shrub environments, *Salix* pollen content was very low, accounting for only 1.40% of the total, while *Betula* and *Alnus* pollens accounted for 49.50% and 15.97%, respectively. Shrub and herb pollen contents (21.56%) were relatively high, including Ericaceae (8.58%).

Table 2 AMS ^{14}C dating results from the Huola Section

Sample	Lab code	Depth (cm)	Sample type	^{14}C ages (yr BP)	δ^{13}C (‰VPDB)	Calibrated ^{14}C ages (cal yr BP)
GLS-10	OZQ790	19	Charcoal	120±40	–29.0	9–151
GL-021	OZQ789	121	Charcoal	3590±40	–25.0±0.1	3823–3988
GL-030	OZQ787	139	Charcoal	3565±40	–26.0±0.2	3813–3975
GL-041	OZQ786	161	Charcoal	5780±45	–25.0	6453–6675
GL-054	OZQ785	187	Charcoal	7050±40	–25.1±0.3	7819–7958

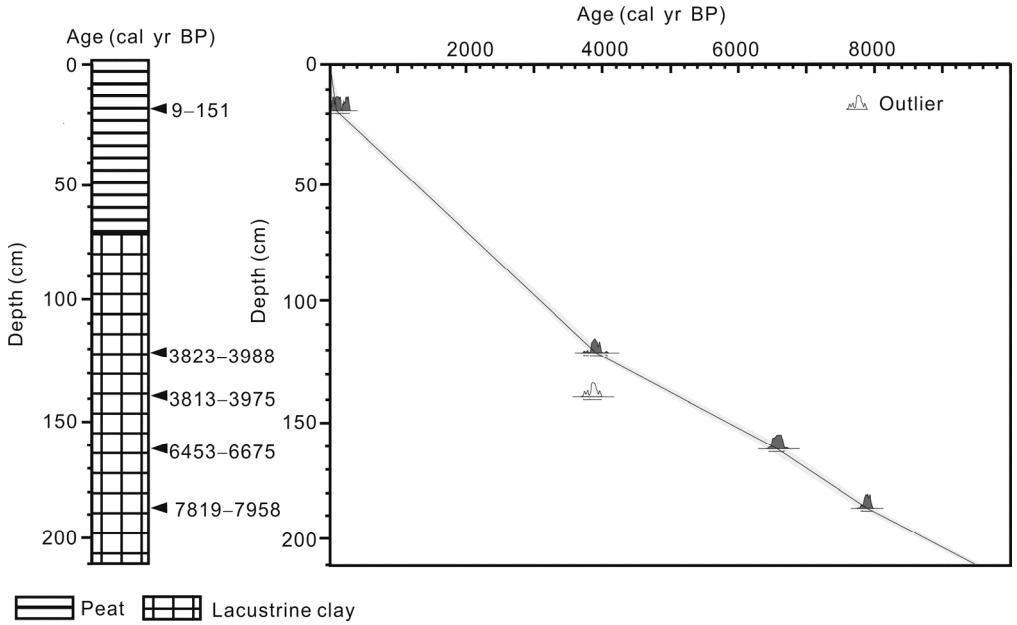

Figure 2 Huola Section and age-depth model.

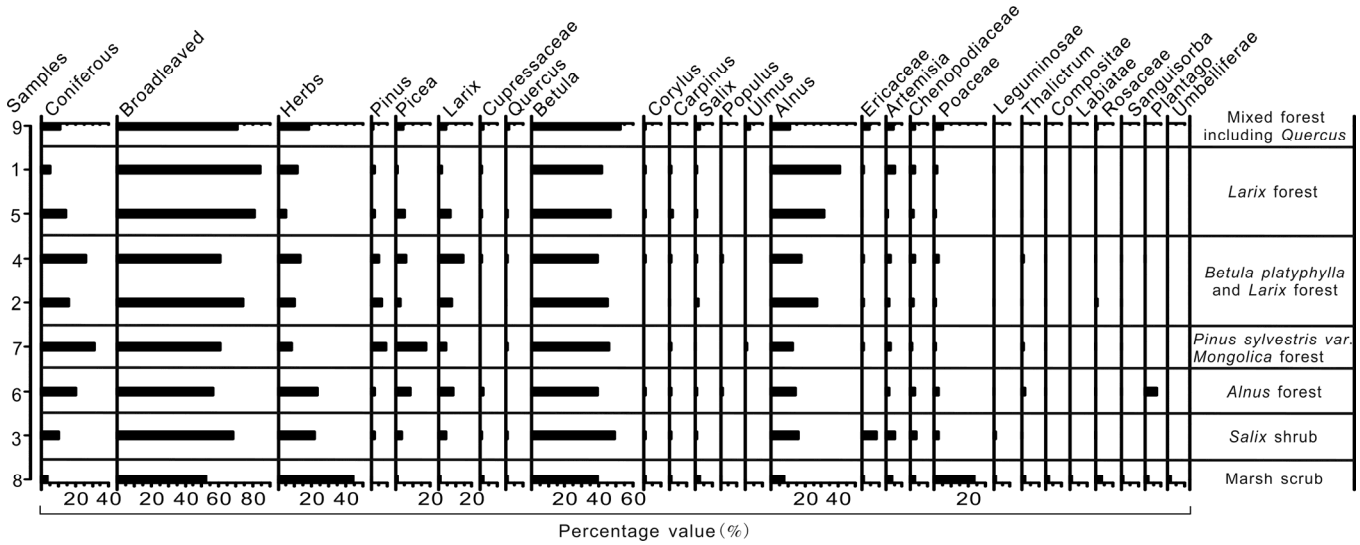

Figure 3 Modern pollen percentages for seven different vegetation types in the northern GKR.

In wetland shrub, shrub and herb pollen percentages reached 44.63%, with relatively high Poaceae (23.66%), Rosaceae (4.36%) and Ericaceae (1.74%) pollen contents. Broadleaved trees (52.01%) and coniferous arbor pollen (3.36%) percentages decreased, of which *Betula* was 38.93%, *Alnus* 7.55%, and *Larix* 1.74%.

In surface pollen assemblages from seven different vegetated environments in the northern GKR, *Betula*, *Alnus*, *Larix*, *Picea*, *Quercus*, *Salix*, Ericaceae, Poaceae and Rosaceae predominated. *Betula* and *Alnus* appeared in every sample, with relatively high contents. Arboreal pollen content was usually >60%, falling to about 55% only in wetland shrub. The existence of birch forests was thus indicated only when the *Betula* content exceeded 40%. In alder shrub areas, *Alnus* pollen content was usually >10%. *Larix* pollen content was clearly lower than its actual presence within the plant community: any paleovegetation reconstruction must take careful note that its pollen content accounted for only 14.68% in larch forest. It also shows that *Betula* pollen is overrepresented and *Larix* pollen is less representative based on the research from east of this area (Yu et al., 2012). Willow shrub topsoil contained relatively high levels of *Salix* (1.4%) and Ericaceae (8.58%), and can thus be distinguished from other vegetation types. A higher proportion of Poaceae (23.66%) was the main characteristic of areas of wetland shrub.

4.2 Pollen assemblages in the Huola Section

58 families and genera of pollen were identified in the Huola Section. Broadleaf tree pollen peaked at 87.3%, of which *Betula* pollen was the commonest, with content ranging from 35.4% to 78.3%. Total pollen concentration ranged from 3.9×10^4 to 2.4×10^6 grains/g.

Six pollen zones can be recognized from pollen assemblages (Figure 4).

Zone 1 (210–190 cm, 9100–8000 cal yr BP): *Betula*, *Larix*, Cupressaceae, *Carpinus*, *Corylus*, *Alnus*, and other tree pollen dominate pollen assemblages (56.27–75.99%). Percentages for broadleaved trees, especially *Betula* pollen (35.18–53.33%), were extremely high. Coniferous tree pollen content, mainly *Larix* (0.67–4.26%) and Cupressaceae pollen (1.67–5.56%), was relatively low (3.83–10.74%). Shrub and herb pollen percentages fluctuated from 24.01% to 43.73%, and were dominated by Poaceae pollen (10.12–27.57%), with relatively high *Artemisia* (4.63–10.12%) and Ericaceae (1.34–3.67%) pollen contents. Total pollen concentrations (3.3×10^5–3.5×10^6 grains/g) were relatively high, with some fluctuation. This zone is thus dominated by CBM forest.

Zone 2 (190–153 cm, 8000–6000 cal yr BP): the spectra are dominated by *Betula*, *Larix*, Cupressaceae, *Picea*, *Pinus*, *Carpinus*, *Corylus*, *Alnus* and other tree pollens, with their total content ranging from 73.74% to 78.74%. Coniferous tree pollen percentages, especially of *Picea* and *Pinus*, increase, peaking at 7300 cal yr BP. In contrast, shrub and herb pollen content (21.26–26.26%) decreases markedly than Zone 1, with Poaceae pollen percentages noticeably dropping (9.69–14.48%). Total pollen concentrations (2.4×10^5–3.5×10^6 grains/g) remain relatively high, suggesting a region of CBM forest accompanied by increasing areas of wet coniferous forest.

Zone 3 (153–137 cm, 6000–5000 cal yr BP): broadleaved tree pollen dominate the pollen spectra, fluctuating from 60.49% to 73.50%. *Betula* (50.88–58.88%) increases, while *Corylus* (1.76–5.57%) and *Carpinus* (2.08–3.72%) sharply decrease. Coniferous tree pollen percentages (5.01–10.57%) clearly decrease, whereas herb content (19.94–34.51%) increases slightly. *Artemisia* (6.25–9.88%) and Ericaceae (2.35–16.24%) increased markedly, while the Poaceae pollen percentage (10.86–3.37%) falls. Total pollen concentrations rise (1.9×10^6–4.1×10^6 grains/g). Pollen records reveal *Larix*- and *Betula*-dominated CBM forests with Ericaceae and *Artemisia* shrubs as undergrowth.

Zone 4 (137–83 cm, 5000–2500 cal yr BP): this zone is characterized by high percentages (59.70–73.50%) of *Betula*, *Corylus*, *Carpinus*, *Alnus* and other broadleaved tree pollens. Among them, *Corylus* (1.94–10.03%) and *Carpinus* (2.07–10.69%) showed little increase. Coniferous tree (*Picea*, *Larix* and *Pinus*) pollen markedly increased (6.07–20.90%), while herb pollen content (12.48–24.43%) decreased noticeably. Some Ericaceae (0.53–2.93%) and Poaceae pollen (1.98–7.89%) were replaced by *Artemisia* pollen (4.50–10.37%). Total pollen concentration peaked at 5.8×10^5–4.6×10^6 grains/g. Pollen assemblages indicated CBM forest, with *Corylus*, *Carpinus* and other small broadleaved trees dominating the vegetation types.

Zone 5 (83–30 cm, 2500–500 cal yr BP): there was a prominent increase in the *Betula* pollen percentage (50.46–67.01%), while *Corylus* (0.30–3.68%), *Carpinus* (0.53–2.87%) and coniferous tree pollen contents (3.51–14.61%) decreased markedly. Ericaceae (1.43–7.61%), Poaceae (1.91–8.87%) and *Sanguisorba* (0.18–1.58%) made relatively sizeable increases. Total pollen concentration (9.5×10^4–2.4×10^6 grain/g) decreased. Pollen assemblages

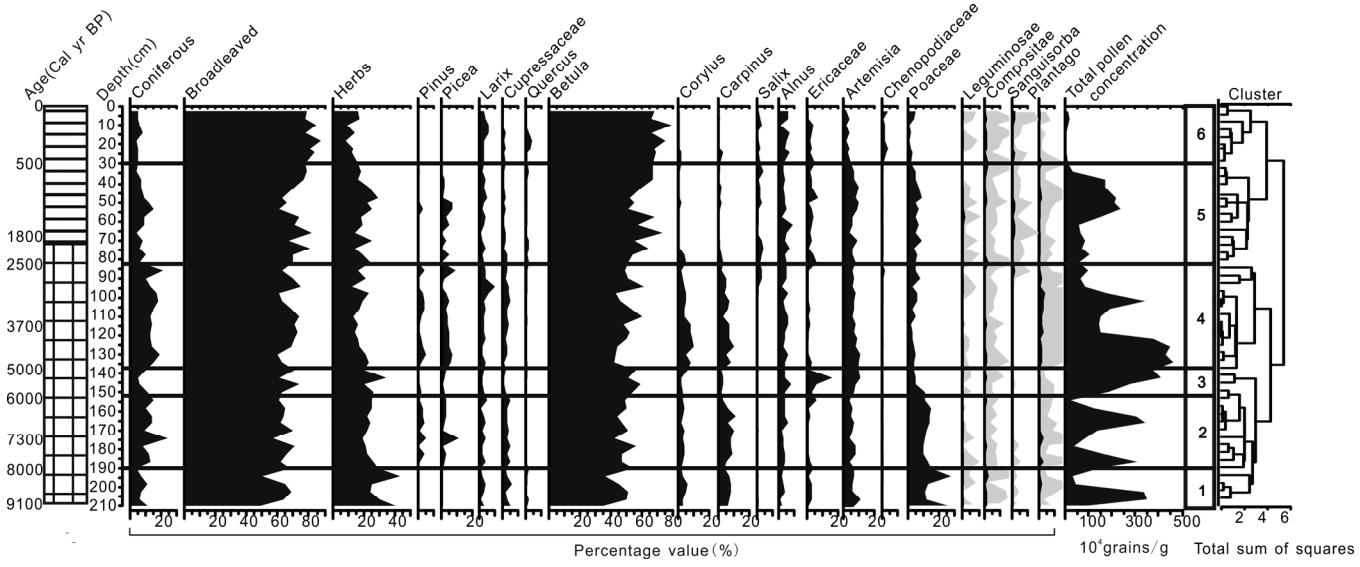

Figure 4 Pollen percentages and concentrations for the Huola Section. The gray values to the right are magnified tenfold to emphasize changes in the percentages of the less abundant taxa.

were characterized by abundant *Betula* forest, with Ericaceae, *Artemisia* and *Sanguisorba* shrub and herb clear in the undergrowth, and CBM forest continuing to develop in the surrounding regions.

Zone 6 (30–0 cm, 500 cal yr BP to present): broadleaf tree pollens (77.13–87.25%), especially *Betula* pollen content (65.47–78.34%), reached their peak value, with some emergence of *Quercus* (0–3.80 %). *Corylus* (0.25–1.88%) and *Carpinus* (0–3.52%) fell to their lowest values. Coniferous tree pollens (4.25–8.3%) decreased, with *Pinus* and *Picea* pollen contents extremely low (<0.45%), while *Larix* pollen increased slightly. Shrub and herb pollen percentages (8.50–17.48%) decreased, but drought-tolerant species like Chenopodiaceae (1.29–3.88%) and Compositae (0.47–1.80%) increased to some extent. Total pollen concentration (3.9×10^4–1.8×10^5 grains/g) reduced significantly. The pollen assemblages indicate *Betula*-dominated open forest, with some *Larix* conifer forest and *Quercus*. In addition, Ericaceae, Chenopodiaceae and Compositae shrubs grew in the undergrowth.

Generally-speaking, the Huola Basin has experienced six chronosequences since 9100 cal yr BP: (1) 9100–8000 cal yr BP, warm-type CBM vegetation, with *Carpinus*, *Corylus* and Poaceae as principal pollen indicators; (2) 8000–6000 cal yr BP, warm-type CBM vegetation, with *Carpinus*, *Corylus*, *Pinus* and *Picea* as principal pollen indicators; (3) 6000–5000 cal yr BP, *Betula*- and *Larix*-dominated CBM forest, with *Betula*, *Larix* and Ericaceae as the main pollen indicators; (4) 5000–2500 cal yr BP, warm-type CBM vegetation, with *Carpinus*, *Corylus*, *Pinus*, *Picea* and *Artemisia* as the main pollen indicators; (5) 2500–500 cal yr BP, cold-temperate CBM forest, with *Betula*, *Larix*, *Sanguisorba* and Ericaceae as principal pollen indicators, and a decrease in total pollen concentrations; and (6) 500 cal yr BP to the present, cold-temperate CBM vegetation, with *Betula*, *Larix*, *Quercus*, Chenopodiaceae and Compositae as the main pollen indicators, and falls in total pollen concentrations.

Within this framework, there were six periods of rapid change: (1) about 8000 cal yr BP, with *Pinus* and *Picea* increasing, and Poaceae decreasing; (2) about 7300 cal yr BP, when coniferous trees peaked; (3) 6000–5000 cal yr BP, when Ericaceae pollen concentrations reached their highest value; (4) 2500 cal yr BP, when *Corylus*, *Carpinus* and other warm-type broadleaved trees nearly disappeared; (5) 1600 cal yr BP, with conifers increasing, and brush and herbs expanding; and (6) 500 cal yr BP, when *Betula* increased and vegetation coverage decreased.

4.3 PCA results

The first and second principal component (PCA F1 and PCA F2) had eigenvalues of 0.77 and 0.1, explaining 77% and 10% of total variance of pollen data respectively (Figure 5a). The plants that registered the highest positive scores for the first component axis included *Corylus* and *Carpinus*; *Betula* and *Sanguisorba* yielded the lowest scores. Poaceae and Polygonaceae had positive loadings on the second component axis, whereas *Alnus* and *Plantago* had negative loadings.

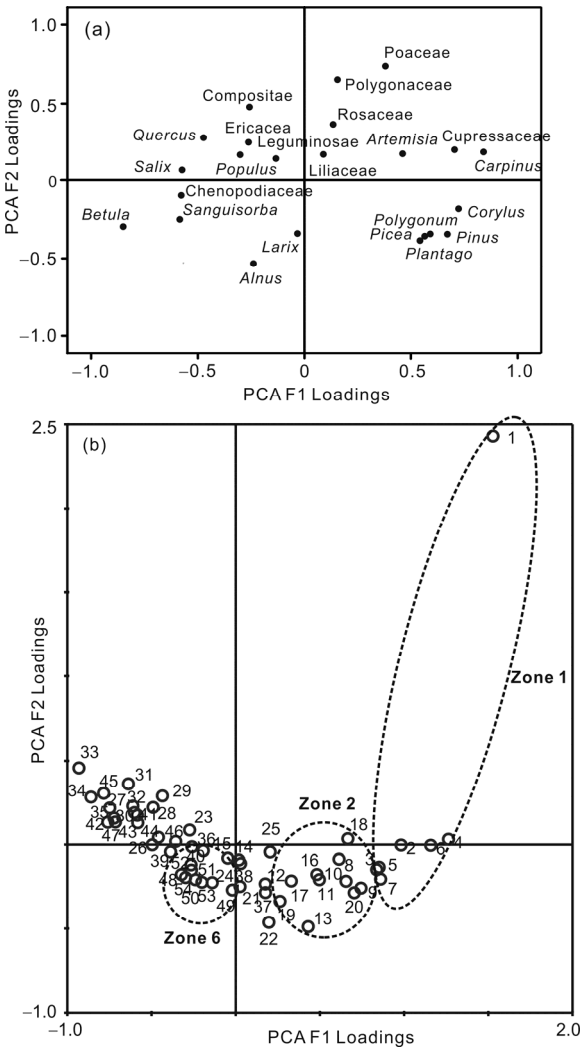

Figure 5 Principal component analysis (PCA) based on pollen species (a) and samples (b) from Huola Section.

According to PCA results of the 53 samples taken from bottom to top of Huola Section (Figure 5b), the score of each sample was distributed regularly on the first and second principal axes of the two-dimensional ordination map. Samples from the six pollen assemblages yielded separately, especially the Zones 1, 2 and 6 displaying individually clusters. However, pollen Zones 3, 4, 5 are close to each other, which might be caused by the high content of *Betula* and *Artemisia* Pollen in the three vegetation types.

5. Discussion

Stalagmite, ice core, ocean and lake sediment records show

that the Holocene experienced increased temperatures in its early stages, a warm-wet mid-Holocene period, and cooling in its later years (Yuan et al., 2004; Wang et al., 2005; Tan et al., 2006). Marcott et al. (2013) have suggested that temperatures during 10000–5000 cal yr BP were 0.7°C warmer than the mid to late Holocene. The Holocene megathermal occurred in the mid-Holocene; the climate about 6000 cal yr BP is indicative of a 1–2°C average increase in global temperatures (Shi et al., 1992; IPCC, 2013). Forest distribution and population density are strongly influenced by climate change (Huntley and Birks, 1983; Bartlein et al., 1986; Fang, 2000); although our results show that different areas responded differently to climate change, there have up until now been no other records sufficiently reliable for testing how the vegetation on the northern margins of the EASM zone in NE China might respond to climate change.

5.1 Climatic implications of Pollen in Huola Basin

Climate change is proven to have a significant impact on terrestrial ecosystems; as a function of this, vegetation types and their spatial migration patterns also change. Surface pollen studies have established that there is a relationship among the pollen percentages as well as vegetation type and regional climate (Odgaard, 1999).

At present, *Corylus* in NE China is mainly distributed in the eastern and southern Zhangguangcai and Changbai Mountain ranges, with *Carpinus* forests principally found in southern Liaoning Province. The average annual rainfall in these areas is about 500–1000 mm and the annual temperature is about 0–8°C (Zhou, 1997). Based on the surface pollen analysis of Huola Basin, a high proportion of Poaceae pollen is the main characteristic of wetland. The increase of precipitation is often accompanied by high abundance of Poaceae pollen in low temperature and high humidity area (Liu et al., 2009).

The distribution of spruce is in cold-temperate zone (average temperature is 0–8°C) in the northern part of NE China, and in the cold-wet subalpine zone at 1000–2000 m (Liu et al., 2009). In these areas, *Picea* pollen abundance generally increases along with the humidity rise (Wu, 1985). The increase of *Pinus* pollen content is used to indicate a higher humidity in semi-arid region, north China (Xiao et al., 2004; Xu et al., 2007). While *Larix gmelinii* and *Betula platyphylla* forests are dominated in cold-temperate zone in the northern GKR, both of which have strong adaptability to cold-dry environment (Zhou, 1997).

Therefore, the PCA F1 and F2 loadings (Figure 5a) reflect the dynamics of vegetation type indicated by pollen record in the study region. The first principal component of PCA better reflected the pollen percentage variations with temperature; that is, *Carpinus* and *Corylus* dominated vegetation types represent a warmer climate, while a high abundance of *Betula* and low PCA F1 scores suggest downward of temperate and thus cold-temperate CBM forest dominated climate conditions. The PCA F2 scores of the taxa on the second principal component indicate changes in humidity, with Poaceae dominated vegetation reflecting a wetter climate, whereas lower values may represent dry conditions (Figure 5b). The PCA F1 and F2 curves thus revealed that temperatures as well as humidity have fluctuated downward since 9100 cal yr BP (Figure 6), in tandem with reductions of insolation in northern hemisphere high latitudes (Berger et al., 1991).

In addition, PCA based on the samples (Figure 5b) reflected a relation between different plant communities and the environment. The first axis may indicate the humidity gradients for different plant communities, with ability to drought strengthening leftward along the axis; the second axis can reflect changes in temperature, with a plant community's ability to withstand cold strengthening downward along the axis. Hence, the environment of Huola Basin might have experienced a main change from warm-wet to cold-dry.

5.2 Vegetation response to climate change

The vegetation succession of the Huola Section in Mohe County shows that, at least about 9100 cal yr BP, this area had well-developed *Larix*, *Picea*, and warm-type broad-leaved (such as *Corylus*, *Carpinus*) CBM vegetation (Figure 4). *Larix* in the Huola Section pollen diagram constitutes a relatively high proportion of the total (0.67–9.63%). Considering the low representativity of *Larix* pollen, it is almost certain that a stable larch community existed in the northern GKR. Therefore, the increases in temperature after 9100 cal yr BP, would have benefited the expansion of *Corylus*, *Carpinus* and developed warm-cold mixed vegetation. Since 8000 cal yr BP, *Pinus*, *Picea* and *Carpinus* increased while Ericaceae and other cold tolerant shrubs decreased (Figure 4).

In order to better reflect the response of vegetation to climate change, the principal pollen percentages, PCA F1, and PCA F2 curves from the Huola Section were compared with high-resolution climate indices from other regions (Figure 6). Results suggested that the warmest and wettest stage in the Holocene occurred at 9100–6000 cal yr BP, when MAT and MAP suited the growth of warmth-loving vegetation in the study area. Using a similar modern climatic index of the vegetation distribution area as a guide, a conservative estimate of early Holocene MAP for Mohe County comes to about 500–600 mm (higher than the modern value 403.4 mm) (Editorial committee of vegetation map of China, Chinese Academy of Sciences, 2007). At about 8000 cal yr BP, *Pinus* and *Picea* forest appeared in the Huola Basin, which may have been due to a stable warm-wet climate.

Many other surveys have produced results which essentially agree with these figures. It shows that deciduous

broadleaved forest developed from the pollen record of Erlongwan Maar Lake in 8900–4600 cal yr BP, which indicated a warm and wet climate (Liu et al., 2008). 9000–2900 cal yr BP, forest-steppe dominated the Moon Lake area in central GKR, and the climate is warmer and wetter than present (Wu et al., 2012). The temperature during 11000–8000 cal yr BP in Hulun Lake in the western GKR reached its highest value in the Holocene (Wen et al., 2010b). The pollen record of Hokkaido Island shows that *Quercus* and other warm-loving broadleaved trees increased markedly in 9000–8000 cal yr BP (Igarashi, 2013). The climate change of Kuril Islands displayed the same trend (Razjigaeva et al., 2013).

It can be inferred from general vegetation succession trends in Mohe County that the local vegetation experienced a transformation from mid-Holocene warm-cold mixed types to late Holocene cold-temperate types: two significant cooling events which had a profound impact on vegetation succession can be identified (Figure 5). At about 6000–5000 cal yr BP, PCA F1 and PCA F2 values drop to a low level. This cooling event may have global parallels, such as the significant ice event identified in North Atlantic records (Bond et al., 1997); stalagmite oxygen isotopes from Dongge Cave also indicate that the EASM became weaker (Dykoski et al., 2005). In addition, this cooling event appears in the Central Asian Lake Baikal Bugulderka core (Tarasov et al., 2007), Jingpo Lake in NE China (Li et al., 2011), Moon Lake (Wu et al., 2012) and Hokkaido Island, Japan (Igarashi and Zharov, 2011). The main driving force for this might have been a weakening in solar activity (Reimer et al., 2004). The vegetation in Mohe area experienced that warm-type trees decreased in number, the Ericaceae percentage reached its peak (Figure 6), and understory grass changed from Poaceae to *Artemisia* (Figure 4). Hence, this cooling event had a widespread and profound influence on NE China.

5000–4000 cal yr BP, global temperature went up again (Shi et al., 1992), and was slightly higher than the modern temperature. Pollen records, including those from the Huola Basin, show that following this event, different areas experienced different vegetation recovery rates as warm and humid conditions developed. With the weakening of northern hemisphere insolation radiation as well as the EASM since 5000 cal yr BP (Berger and Loutre, 1991; Dykoski et al., 2005; Wang et al., 2005), the precipitation reduced in Huola Basin, and drought tolerant *Artemisia* shrubs instead of Poaceae grown under the forests, indicating a warm and dry environments.

At about 3500–2500 cal yr BP, vegetation in the Mohe area, previously dominated by warm-temperate trees, was gradually replaced by cold-temperate type vegetation. This transformation came to an end around 2500 cal yr BP when PCA F1 value drops to a lower level (Figure 6): *Corylus*, *Carpinus* and other warm-type broadleaf trees had all but disappeared, while *Betula*, *Larix* and other cold- temperate

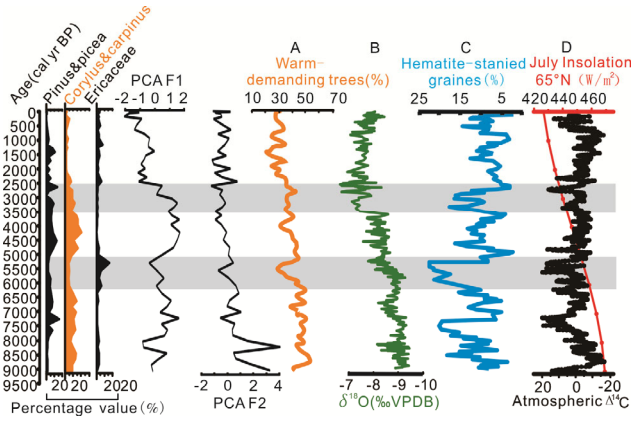

Figure 6 Comparison of principal pollen percentages and PCA F1 (F2) curve with other selected proxy records from the Northern Hemisphere. From left to right: the first panel shows the age/depth relation; the second panel shows the summed percentages for *Pinus* and *Picea* pollen, and for *Corylus* and *Carpinus* pollen, the percentage of *Betula* and Ericaceae pollen, PCA F1 curve, and PCA F2 curve. A, warm-responsive tree pollen percentages (five point moving average) (Li et al., 2011); B, Dongge Cave D4 (Dykoski et al., 2005); C, Holocene drift ice record for the MC52-VM29-191 North Atlantic core (Bond et al., 1997); D, Northern Hemisphere July insolation at 65°N (Berger and Loutre, 1991), and the residual atmospheric $\Delta^{14}C$ record (about 2000 year moving average) (Reimer et al., 2004). The lateral grey bands trace the interconnection between climate cooling, a strengthened EASM, meltwater, and reduced insolation activity.

type forests dominated, with increases in *Salix*, Ericaceae, *Sanguisorba* and Chenopodiaceae thicketization. This event at about 2500 cal yr BP also appears in other records, such as those from Hulun Lake (Wen et al., 2010b), Moon Lake (Wu et al., 2012), Dali Lake (Xiao et al., 2008), Gushantun Bog (Liu, 1989), Jingpo Lake (Li et al., 2011), and Hokkaido Island (Igarashi and Zharov, 2011; Razjigaeva et al., 2013). These tend to indicate that the cooling might have been caused by a weakening of Northern Hemisphere summer insolation radiation (Berger and Loutre, 1991; Dykoski et al., 2005). In addition, the time lag between abrupt cooling event during 3500–2500 cal yr BP and the vegetation conversion in Huola Basin, might possibly owing to various reasons, such as topographic factors, small climatic oscillation. After 500 cal yr BP, the PCA F1 drops to the lowest value, spruce forest declined further, and the current vegetation pattern arose (Figure 6).

The Holocene megathermal provides important pointers toward the likely future effect of a warming climate on the vegetation and ecological environment of the study area (Kutzbach et al., 1996; Berthel et al., 2012; Liu et al., 2013). The Holocene megathermal in Huola Basin occurred at about 9100–6000 cal yr BP, when increases in MAT and MAP provided conditions suited to the growth of warm-type coniferous and broadleaved forests. This provides the clearest evidence of vegetation succession in the Holocene. Our study of this period suggests that such warming could have resulted in a strengthening of the EASM's influence on northernmost NE China, which would

have benefited the development of warm-temperate forest vegetation and an improved plant load.

6. Conclusions

There was a clear relation between topsoil pollen combinations and vegetation types in the northern GKR. *Betula* and *Alnus* pollen percentages are the most indicative of the existence of vegetation; the *Betula* pollen takes more than 40% in birch forest topsoil, and more than 14% *Alnus* pollen indicates alder forest. *Larix* pollen (14.68%) is less representative of the existence of larch forest.

The Holocene warm period in NE China (9100–6000 cal yr BP), with its increases in temperature, represents the Holocene stage most conducive to the development of warm-type forest vegetation and an improved plant load, with a growth in *Carpinus*- and *Corylus*-dominated temperate CBM forest.

Two cooling events, at 6000–5000 cal yr BP and 3500–2500 cal yr BP, facilitated a transition from warm-type vegetation such as *Corylus*, *Carpinus*, *Pinus* and *Picea* to cold-type *Larix* and *Betula* forest. After 2500 cal yr BP, *Larix* and *Betula* dominated the cold-temperate vegetated landscape.

Acknowledgements *We thank Liu Hanbin, Gao Qiang and Lin Lin for assistance with fieldwork as well as the sample analysis. The authors thank the two anonymous reviewers for their constructive comments and suggestions. This research was supported by the Chinese Academy of Sciences (CAS) Strategic Priority Research Program (Grant No. XDA01020304), the National Natural Science Foundation of China (Grant No. 41372175), the National Basic Research Program of China (Grant No. 2015CB953803), and the Special Fund Project of the Ministry of Land and Resources for Scientific Research into Public Welfare (Grant No. 201311137).*

References

An Z S, Porter S C, Kutzbach J E, Wu X H, Wang S M, Liu X D, Li X Q, Zhou W J. 2000. Asynchronous Holocene optimum of the East Asian monsoon. Quat Sci Rev, 19: 743–762

Bartlein P J, Prentice I C, Webb T. 1986. Climatic response surfaces from pollen data for some eastern North American taxa. J Biogeogr, 13: 35–57

Berger A, Loutre M F. 1991. Insolation values for the climate of the last 10 million years. Quat Sci Rev, 10: 297–317

Berthel N, Schwörer C, Tinner W. 2012. Impact of Holocene climate changes on alpine and treeline vegetation at Sanetsch Pass, Bernese Alps, Switzerland. Rev Palaeobot Palynol, 174: 91–100

Bond G, Showers W, Cheseby M, Lotti R, Almasi P, Menocal P D, Priore P, Cullen H, Hajdas I, Bonani G. 1997. A pervasive millennial-scale cycle in North Atlantic Holocene and Glacial Climates. Science, 278: 1257–1266

Chen Y F. 1997. Research on responses of vegetation to climate change. Prog Geog, 16: 70–77

Ding Z L, Duan X N, Ge Q S, Zhang Z Q. 2010. On the major proposals for carbon emission reduction and some related issues. Sci China Earth Sci, 53: 159–172

Dykoski C A, Edwards R L, Cheng H, Yuan D X, Cai Y J, Zhang M L, Lin Y S, Qing J M, An Z S, Revenaugh J. 2005. A high-resolution, absolute-dated Holocene and deglacial Asian monsoon record from Dongge Cave, China. Earth Planet Sci Lett, 233: 71–86

Editorial committee of vegetation map of China, Chinese Academy of Sciences. 2007. Vegetation Map of the People's Republic of China (1∶1000000). Beijing: Geological Publishing House. 263

Erdtman G. 1960. The acetolysis method: A revised description. Svensk Bot Tidsk, 54: 561–564

Fang J Y. 2000. Global Ecology: Climate Change and Ecological Responses. Beijing: Higher Education Press. 218

Feagri K, Iversen J. 1989. Textbook of Pollen Analysis. 3rd ed. Oxford: Blackwell. 295

Feng J S. 1979. The origin of the Oroqen nationality. J Northeast Normal Univ, 2: 77–85

Gao C Y, Bao K S, Lin Q X, Zhao H Y, Zhang Z Q, Xing W, Lu X G, Wang G P. 2014. Characterizing trace and major elemental distribution in late Holocene in Sanjiang Plain, Northeast China: Paleoenvironmental implications. Quat Int, 349: 376–383

Guo D X, Huang Y Z, Wang J C, Wang B L, Zeng Z G, He Y X, Yang D W, Liu R S. 1989. Function of geologic structure in the formation of permafrost conditions in Huola river basin, North Da Hinggan Ling. J Glaciol Geocryol, 11: 215–222

Guo D X, Wang S L, Lu G W, Dai J B, Li E Y. 1981. Division of permafrost regions in Daxiao Hinggan Ling northeast China. J Glaciol Geocryol, 3: 1–9

Guo Z X, Zhang X N, Wang Z M, Fang W H. 2010. Responses of vegetation phenology in Northeast China to climate change. Chin J Ecol, 29: 578–585

Hong B, Liu C Q, Lin Q H, Shibata Y, Leng X T, Wang Y, Zhu Y X, Hong Y T. 2009. Temperature evolution from the δ^{18}O record of Hani peat, Northeast China, in the last 14000 years. Sci China Ser D-Earth Sci, 52: 952–964

Hong Y T, Hong B, Lin Q H, Shibata Y X, Zhu Y X, Leng X T, Wang Y. 2009. Synchronous climate anomalies in the western North Pacific and North Atlantic regions during the last 14000 years. Quat Sci Rev, 28: 840–849

Huntley B, Birks H J B. 1983. An Atlas of Past and Present Pollen Maps for Europe: 0–13000 B.P. Cambridge: Cambridge University Press

Igarashi Y. 2013. Holocene vegetation and climate on Hokkaido Island, northern Japan. Quat Int, 290: 139–150

Igarashi Y, Zharov A E. 2011. Climate and vegetation change during the late Pleistocene and early Holocene in Sakhalin and Hokkaido, northeast Asia. Quat Int, 237: 24–31

Intergovernmental Panel on Climate Change (IPCC). 2013. Climate Change 2013: The Physical Sciences Basis. New York: Cambridge University Press. 996

Jiang W Y, Leroy S A G, Ogle N, Chu G Q, Wang L, Liu J Q. 2008. Natural and anthropogenic forest fires recorded in the Holocene pollen record from a Jinchuan peat bog, northeastern China. Paleogeogr Paleoclimatol Paleoecol, 261: 47–57

Kröpelin S, Verschuren D, Lézine A-M, Eggermont H, Cocquyt C, Francus P, Cazet J P, Fagot M, Rumes B, Russell J M, Darius F, Conley D J, Schuster M, Suchodoletz H V, Engstrom D R. 2008. Climate-driven ecosystem succession in the Sahara: The past 6000 years. Science, 320: 765–768

Kutzbach J, Bonan G, Foley J, Harrison S P. 1996. Vegetation and soil feedbacks on the response of the African monsoon to orbital forcing in the early to middle Holocene. Nature, 384: 623–626

Lan Y. 2002. Chinese Historical Geography. Beijing: High Education Press. 155–156

Li C H, Wu Y H, Hou X H. 2011. Holocene vegetation and climate in Northeast China revealed from Jingbo Lake sediment. Quat Int, 229: 67–73

Li F, Zhou G S, Cao M C. 2006. Responses of *Larix gmelinii* geographical distribution to future climate change: A simulation study. Chin J Appl Ecol, 17: 2255–2260

Li Q, Wang W W, Chen W Y. 2010. Underground ice characteristics and causes discussion of Yueya Lake in Huola coalfield basin Mohe County, Heilongjiang Province. Jilin Geol, 29: 120–126

Li X Q, Du N Q. 1999. The acid-alkali-free analysis of Quaternary pollen. Acta Bot Sin, 41: 782–784

Li X Q, Zhao H L, Yan M H, Wang S Z. 2005. Fire variations relationship

among fire and vegetation and climate during Holocene at Sanjiang Plain, Northeast China. Sci Geogr Sin, 25: 177–182
Liu H Y, Williams A P, Allen C D, Guo D L, Wu X C, Anenkhonov O A, Liang E, Sandanov D V, Yin Y, Qi Z H, Badmaeva N K. 2013. Rapid warming accelerates tree growth decline in semi-arid forests of Inner Asia. Glob Change Biol, 19: 2500–2510
Liu J L. 1989. Vegetational and climatic changes at Gushantun bog in Jilin Province, NE China since 13000 year BP. Acta Palaeontol Sin, 28: 495–511
Liu Q, Li Q, Wang L, Chu G Q. 2010. Stable carbon isotope record of bulk organic matter from a sediment core at Moon Lake in the middle part of the Daxing'an Mountain Range, northeast China during the last 21 ka. Quat Sci, 30: 1069–1077
Liu Y Y, Zhang S Q, Liu J Q, You H T, Han J T. 2008. Vegetation and environment history of Erlongwan Maar Lake during the late Pleistocene on pollen record. Acta Micropalaeontol Sin, 25: 274–280
Mao X M, Cheng S G, Hong Y T, Zhu Y X, Wang F L. 2009. The influence of volcanism on paleoclimate in the northeast of China: Insights from Jinchuan peat, Jilin Province, China. Chin J Geochem, 28: 212–219
Marcott S A, Shakun J D, Clark P U, Mix A C, Clark P U. 2013. A reconstruction of regional and global temperature for the past 11300 years. Science, 339: 1198–1201
Odgaard B V. 1999. Fossil pollen as a record of past biodiversity. J Biogeogr, 26: 7–17
Ramsey C B, Lee S. 2013. Recent and planned developments of the program OxCal. Radiocarbon, 55: 720–730
Razjigaeva N G, Ganzey L A, Grebennikova T A, Belyanina N I, Mokhova L M, Arslanov K A, Chernov S B. 2013. Holocene climatic changes and vegetation development in the Kuril Islands. Quart Int, 290: 126–138
Reimer P J, Bard E, Bayliss A, Beck J W, Blackwell P G, Ramsey C B, Buck C E, Cheng H, Edwards R L, Friedrich M, Grootes P M, Guilderson T P, Haflidason H, Hajdas I, Hatté C, Heaton T J, Hoffmann D L, Hogg A G, Hughen K A, Kaiser K F, Kromer B, Manning S W, Niu M, Reimer R W, Richards D A, Scott E M, Southon J R, Staff R A, Turney C S M, Plicht J V D. 2013. IntCal13 and Marine13 radiocarbon age calibration curves 0–50000 years cal BP. Radiocarbon, 55: 1869–1887
Reimer P J, Baillie M G L, Bard E, Bayliss A, Beck J W, Bertrand C J H, Blackwell P G, Buck C E, Burr G S, Cutler K B, Damon P E, Edwards R L, Fairbanks R G, Friedrich M, Guilderson T P, Hogg A G, Hughen K A, Kromer B, Mccormac G, Manning S, Ramsey C B, Reimer R W, Remmele S, Southon J R, Stuiver M, Talamo S, Taylor F W, Van D P J, Weyhenmeyer C E. 2004. Residual delta ^{14}C around 2000 year moving average of IntCal04. Radiocarbon, 46: 1029–1058
Ren G Y. 1999. Wetness changes of the Holocene in northeast China. Geol Rev, 45: 255–264
Ren G Y. 2000. Decline of the mid- to late Holocene forests in China: Climatic change or human impact? J Quat Sci, 15: 273–281
Ren G Y. 2007. Changes in forest cover in China during the Holocene. Veg Hist Archaeobot, 16: 119–126
Shi Y F, Kong Z C, Wang S M, Tang L Y, Wang F B, Yao T D, Zhao X T, Zhang P Y, Shi S H. 1992. The climate variation and important events during Holocene Megethemal in China. Sci China Ser B, 22: 1300–1308
Stebich M, Mingram J, Han J T, Liu J Q. 2009. Late Pleistocene spread of (cool-)temperate forests in Northeast China and climate changes synchronous with the North Atlantic region. Glob Planet Change, 65: 56–70
Tan M, Baker A, Genty D, Smith C, Esper J, Cai B. 2006. Applications of stalagmite laminae to paleoclimate reconstructions: Comparison with dendrochronology/climatology. Quat Sci Rev, 25: 2103–2117
Tarasov P, Bezrukova E, Karabanov E, Nakagawa T, Wagner M, Kulagina N, Letunova P, Abzaeva A, Granoszewski W, Riedel F. 2007. Vegetation and climate dynamics during the Holocene and Eemian interglacials derived from Lake Baikal pollen records. Paleogeogr Paleoclimatol Paleoecol, 252: 440–457
Wang B L, Lin F T. 1987. Groundwater in the environment of permafrost at the northern of Da Hinggan Mountains: Take Huola River Basin as an example. Hydrogeol Eng Geol, 5: 5–9
Wang B L, Zhou Y W, Guo D X. 1988. Effects of permafrost on groundwater in Huola Basin, Northern Daxinganling Ridge. J Glaciol Geocyrol, 10: 143–150
Wang L L, Shao X M, Huang L, Liang E Y. 2005. Tree-ring characteristics of *Larix emelinii* and *Pinus sylvestris* var. *mongolica* and their response to climate in Mohe, China. Acta Phytoecol Sin, 29: 380–385
Wang Y J, Cheng H, Edwards R L, He Y Q, Kong X G, An Z S, Wu J Y, Kelly M J, Dykoski C A, Li X D. 2005. The Holocene Asian Monsoon: Links to solar changes and North Atlantic Climate. Science, 308: 854–857
Wen R L, Xiao J L, Chang Z G, Zhai D Y, Xu Q H, Li Y C, Itoh S. 2010a. Holocene precipitation and temperature variations in the East Asian monsoonal margin from pollen data from Hulun Lake in northeastern Inner Mongolia, China. Boreas, 39: 262–272
Wen R L, Xiao J L, Chang Z G, Zhai D Y, Xu Q H, Li Y C, Itoh S, Lomtatidze Z. 2010b. Holocene climate changes in the mid-high-latitude-monsoon margin reflected by the pollen record from Hulun Lake, northeastern Inner Mongolia. Quat Res, 73: 293–303
Wu J, Liu Q. 2012. Charcoal-recorded climate changes from Moon Lake in Late Glacial. Chin J Geol, 37: 947–954
Wu X C, Liu H Y, Guo D L, Anenkhonov O A, Badmaeva N K, Sandanov D V. 2012. Growth Decline Linked to Warming-Induced Water Limitation in Hemi-Boreal Forests. PloS One, 7: e42619
Wu X H. 1985. A study of palaeotemperatures recorded by the Pleistocene Picea-Abies floras in east and southwest China. Bull Inst Geomech CAGS, 6: 155–166
Wu Z Y. 1979. Zoning of flora in China. Acta Bot Yunnan, 1: 1–20
Xia Y M. 1996. Study on record of spore-pollen in high Moor peat and development and successive process of peat in Da and Xiao Hinggan Mountains. Sci Geogr Sin, 16: 337–344
Xiao J L, Si B, Zhai D Y, Itoh S, Lomtatidze Z. 2008. Hydrology of Dali Lake in central-eastern Inner Mongolia and Holocene East Asian monsoon variability. J Paleolimnol, 40: 519–528
Xiao J L, Xu Q H, Nakamura T, Yang X L, Liang W D, Inouchi Y. 2004. Holocene vegetation variation in the Daihai Lake region of north-central China: a direct indication of the Asian monsoon climatic history. Quat Sci Rev, 23: 1669–1679
Xu D K, Lu H Y, Chu G Q, Wu N Q, Shen C M, Wang C, Mao L M. 2014. 500-year climate cycles stacking of recent centennial warming documented in an East Asian pollen record. Sci Rep, 4: 3611
Xu Q H, Tian F, Bunting M J, Li Y C, Ding W, Cao X Y, He Z G. 2012. Pollen source areas of lakes with inflowing rivers: Modern pollen influx data from Lake Baiyangdian, China. Quat Sci Rev, 37: 81–91
Yu S H, Zheng Z, Huang K Y, Skrypnikova M I. 2012. Modern pollen distribution in the Heilongjiang-Amur cold temperate regions of China and Russia. Acta Palaeontol Sin, 51: 370–384
Yuan D X, Cheng H, Edwards R L, Dykoski C A, Kelly M J, Zhang M L, Qing J M, Lin Y S, Wang Y J, Wu J Y, Dorale J A, An Z S, Cai Y J. 2004. Timing, duration, and transitions of the last interglacial Asian monsoon. Science, 304: 575–578
Zhang S Q, Deng W, Yan M H, Li X Q, Wang S Z. 2004. Pollen record and forming process of the peatland in late Holocene in the north bank of Xingkai Lake, China. Wetland Sci, 2: 110–115
Zhao Y, Yu Z C, Chen F H, Zhang J W, Yang B. 2009. Vegetation response to Holocene climate change in monsoon-influenced region of China. Earth-Sci Rev. 97: 242–256
Zhao Y, Herzschuh U. 2009. Modern pollen representation of source vegetation in the Qaidam Basin and surrounding mountains, north-eastern Tibetan Plateau. Veg Hist Archaeobot, 18: 245–260
Zheng Z, Huang K Y, Xu Q H, Lu H Y, Cheddadi R, Luo Y L, Beaudouin C, Luo C X, Zheng Y W, Li C H, Wei J H, Du C B. 2008. Comparison of climatic threshold of geographical distribution between dominant plants and surface pollen in China. Sci China Ser D-Earth Sci, 51: 1107–1120
Zhou Y L. 1997. Geography of the Vegetation in Northeast China. Beijing: Science Press. 30–38
Zhu J Y, Mingram J, Brauer A. 2013. Early Holocene aeolian dust accumulation in northeast China recorded in varved sediments from Lake Sihailongwan. Quat Int, 290: 299–312
Zhu S G. 1992. Vegetation changes during the history in northeast China. J Chin Hist Geo, 4: 105–119